

Investigating Interactions of Biomembranes and Alcohols: A Multiscale Approach

Allison N. Dickey
Roland Faller *

Department of Chemical Engineering & Materials Science,
UC Davis, Davis, CA 95616, USA

October 23, 2018

Abstract

We study the interaction of lipid bilayers with short chain alcohols using molecular dynamics on different length scales. We use detailed atomistic modeling and modeling on the length scale where an alcohol is just an amphiphilic dimer. Our strategy is to calibrate a coarse-grained model against the detailed model at selected state points at low alcohol concentration and then perform a wider range of simulations using the coarse-grained model. We get semiquantitative agreement with experiment for the major observables such as order parameter and area per molecule. We find a linear increase of area per molecule with alcohol concentration. The alcohol molecules in both system descriptions are in close contact with the glycerol backbone. Butanol molecules can enter the bilayer to some extent in contrast to the behavior of shorter alcohols. At very high alcohol concentrations we find clearly increased interdigitation between leaflets.

1 Introduction

Phospholipid bilayers serve an important role in all living cells since they constitute the bulk of cellular and intracellular membranes. Therefore, it is not surprising that there is significant attention and research devoted to the exploration of phospholipid behavior. Computer simulations play an ever increasing role in this field. Detailed computer simulations of phospholipid monolayers and bilayers have recently achieved a high degree of sophistication [1–10]. The interactions between lipid bilayers and water have been thoroughly examined and these investigations have resulted in refined bilayer structural models [5,7,11,12]. Mixtures of various phospholipids [12–15] as well as of phospholipids and cholesterol

*to whom correspondence should be addressed at rfaller@ucdavis.edu

systems [16–19] have been recently characterized. However, the interactions between lipid bilayer membranes and small molecules have not gained much attention except for a few initial studies with alcohols [20–22], sugars [23, 24], and dimethylsulfoxide (DMSO) [25, 26].

Since cell membranes are the first part of the cell to contact with any nutrient or pathogen in the extracellular matrix, it is extremely important to fully understand membrane interactions with biologically relevant small molecules.

It has been experimentally observed that alcohols have a destabilizing effect on model membranes [27, 28] by causing an increase in area per molecule and a decrease in bilayer thickness. This alcohol induced change in bilayer structure is directly related to the industrial problem of stuck fermentation in the wine industry [29, 30]. A stuck fermentation occurs when yeast cells do not transform all available sugar into alcohol. It has been proposed that the underlying mechanism of this problem is an alcohol-triggered structural transition in the membrane. This results in a conformational change in trans-membrane proteins and causes the proteins to become dysfunctional [29]. To date, there is no available method for predicting a stuck fermentation. By examining the influence of alcohols, such as butanol, on lipid bilayers, we will be able to study the primary mechanisms that cause stuck fermentations, as protein conformational changes are predicted to be a secondary effect.

To determine how the entire bilayer area is affected by interactions with n-butanol molecules, a multiscale approach is used. Coarse-grained simulations can be used to study large scale fluctuations and membrane curvature (on the order of tens of nanometers). Detailed atomistic simulations on the scale of a few angstroms are appropriate for studying interactions between neighboring atoms. Surprisingly, biomembrane multiscale models are not as abundant as polymer multiscale models. There have been a few proposed coarse-grained models [31–40] and they have the advantage of being economical in computer power because a number of atoms or even whole molecules are combined into fictitious units and are assigned an interaction potential. This potential is often designed to be computationally efficient rather than an accurate system representation. However, generic chemical effects such as hydrophilic–hydrophobic interactions [34], or the anisotropy of the overall molecule [33] are usually included in the potential. Even though the atomistic detail is missing, interesting generic properties of membranes have been elucidated with these models. One example is the general pathway of self-assembly, which is not specific to the individual lipid [33–35].

The purpose of this contribution is to study the effects of low molecular weight alcohols, such as n-butanol, by combining a fully atomistic model with a recently proposed coarse-grained model [40, 41].

2 Simulation Techniques

We used molecular dynamics simulations to investigate the interactions between phospholipid bilayers and n-butanol at varying alcohol concentrations. Both

an atomistic-scale and coarse-grained model were used. All simulations were performed at 325 K and atmospheric pressure (1 atm). The simulated membranes consisted of fully hydrated dipalmitoylphosphatidylcholine (DPPC) bilayers with 128 molecules, i.e., 64 per leaflet. DPPC was chosen because it is one of the most abundant phospholipids in animal cell membranes. We performed our simulations for both scales using the GROMACS simulation suite [42].

2.1 Atomistic Modeling

Our detailed simulations are fully atomistic with an exception for hydrogen atoms that are bonded in methyl(ene) groups both in butanol as well as in the lipid tails. These hydrogens together with the respective carbon are collapsed into one united atom description. Simulations of the pure bilayer, as well as bilayers with up to 5 wt% n-butanol, (lipid free basis, as we do not take the lipids into account for concentration calculations) have been performed. Simulations were performed under constant temperature and constant pressure conditions using the Berendsen weak-coupling scheme [43]. The coupling times were $\tau_p = 1.0$ ps and $\tau_T = 0.2$ ps for pressure and temperature respectively and a compressibility of 1.12×10^{-6} atm⁻¹. The simulations with a time-step of 2 fs lasted up to 10 ns. We used a cutoff of the Lennard-Jones interaction of 1.0 nm. The lipid simulation models were designed by Berger *et al.* [44]. Additionally, we use the Gromos model for alcohols [42] combined with the SPC/E model [45] for water. Electrostatic interactions have been considered using the particle mesh Ewald technique [46]. The initial system configurations were taken from earlier studies on shorter alcohols [47] where the ethanol was replaced by n-butanol.

2.2 Coarse-Grained Modeling

For the coarse-grained simulations our water and lipid interaction potential parameters come from a model proposed by Marrink *et al* [40] [40]. The initial system configurations were deduced from an earlier study on pure DPPC [40]¹. The model was originally parameterized to reproduce the structural, dynamic, and elastic properties of both lamellar and non-lamellar phospholipid states. Groups of 4–6 heavy atoms are combined into coarse-grained interaction sites and are classified according to their hydrophobicity. The lipid headgroup consists of four sites. There are two hydrophilic sites: one representing the choline and one representing the phosphate group, and two intermediately hydrophilic sites capable of hydrogen bonding representing the glycerols. Each of the two DPPC tails is modeled by four hydrophobic sites. Water is represented by hydrophilic interaction sites, where each site represents four real water molecules. All sites interact in a pairwise manner via a Lennard-Jones (LJ) potential. Five different LJ potentials are used and range from weak for hydrophobic interactions to strong for hydrophilic interactions.

¹Model and configurations available for download at <http://md.chem.rug.nl/~marrink/coarsegrain.html>

In addition to the LJ interactions, a screened Coulomb interaction is used to model the electrostatic interaction between the zwitterionic headgroups. The choline group bears a charge of +1, and the phosphate group bears a charge of -1. Soft springs between bonded pairs keep the molecules intact. Angle potentials provide the appropriate chain stiffness and correct conformation. For efficiency reasons all CG atoms have the same mass of 72 atomic units in the simulation.

For our studies, we had to devise a model for the alcohol as it was not defined in the original force-field. We use the strategy explained in the manual [48]. Thus, our alcohols are modeled as a dimer of a hydrophilic site and a hydrophobic site. The hydrophilic site interacts like the water molecules, the hydrophobic site is the same as the alkanes in the lipids. We performed additional simulations where the hydrophilic site was exchanged against an interaction like the one of the glycerols, this did not change the conclusions significantly. We are aware that this model makes the alcohol a symmetric amphiphile which is not fully realistic. As the interaction centers in the lipid tails stand for four carbons we use this coarse-grained alcohol as n-butanol and refer to it that way in the remainder of the article. Note, that we did not do any re-optimization of any parameter. We experimented with slightly different parameterizations but these were not as successful. This may be attempted in subsequent work but here we want to check the quality of the proposed model.

All simulations are set up in the bilayer state and we do not observe any tendency of instability of the bilayer on the timescale of the simulations which lasted for up to $2.4\mu s$. Note, that this is an effective time. A scaling factor of four was previously found to reproduce both lipid lateral diffusion rates and the self-diffusion of water for the CG model [40]. The times reported in this paper will therefore be effective times which are physically meaningful. For example we use a time-step of 40 fs which is considered to represent 160 fs.

The box dimensions are again coupled semi-isotropically to a pressure bath of 1 atm [43]. The temperature of the system is controlled using a weak coupling scheme [43] with coupling times $\tau_p = 1$ ps, $\tau_T = 10$ ps, measured in the rescaled time scale. The compressibility was set to 5×10^{-6} atm⁻¹. The cutoff for Lennard-Jones interactions as well as the electrostatics was $R_C = 1.2$ nm.

The water rescaling is also visible in the alcohol concentrations. Since one CG water represents four water molecules whereas one CG butanol represents one real n-butanol, so that a simulated concentration of 1:100 (butanol : CG water) actually represents 1:400. This renormalization was taken in consistency with the water diffusion, no further change of parameters was applied. Table 1 summarizes all simulations considered in this work and Figure 1 shows snapshots of an atomistic and a coarse-grained simulation in comparison.

3 Results and Discussion

The most important use of a coarse-grained model is that significantly longer time scales can be achieved with this model than if an atomistic model were

System Type	# Alcohols	# Waters	molar concentration
CG	0	1300	0.0
CG	5	1300	0.0010
CG	7	1300	0.0013
CG	10	1300	0.0019
CG	15	1300	0.0028
CG	25	1300	0.0048
CG	50	1300	0.0095
CG	75	1300	0.0142
CG	100	1300	0.0189
ATOM	0	3655	0.0
ATOM	8	3655	0.0021
ATOM	39	3655	0.0105

Table 1: Overview of the simulated systems. ATOM denotes simulations in atomistic detail and CG represents coarse-grained simulations. Note that in the case of coarse-grained simulations the number of coarse grained waters corresponds to 4 times as many real water molecules and is considered correspondingly in the concentrations

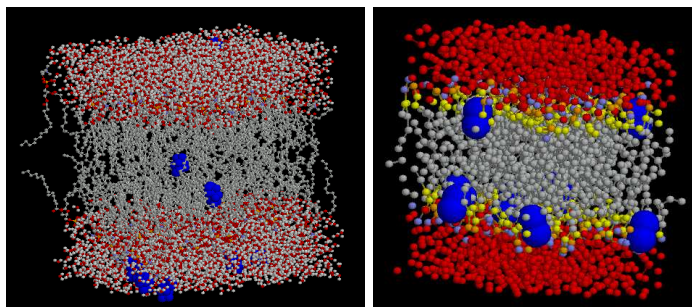


Figure 1: Snapshots: Left: atomistic system with 8 butanols, Right: coarse-grained system with 10 butanols. The two systems are very close to each other in (rescaled) concentration. Butanol molecules are highlighted in blue and increased in size for clarity. Note, that the water in the coarse-grained model are red due to the oxygens.

applied. In our case coarse-grained simulations which were running for 600 ns simulation time ($2.4\mu\text{s}$ effective time) took 40 hours on a AMD Athlon. On the same computer system the atomistic simulations take about 1.5 days for a nanosecond so the speedup is around three orders of magnitude. However, it is important that the coarse-grained model appropriately represents the underlying system. To this end we are comparing a number of important variables. The area per molecule is one of the easiest experimental observables for such a system. It has been measured for n-butanol and other low molecular weight alcohols [27, 28]. The experimental system is not exactly the same as our simulations as it was a SOPC bilayer at $T=298$ K. SOPC is unlike DPPC not fully saturated and both tails are 4 carbons longer, such that quantitative comparisons cannot be made. In the simulations we measure the area per molecule as the area of the system in the xy -plane – the z direction is the bilayer normal – divided by the number of lipids per leaflet (here 64).

Figure 2 shows the dependence of the area per molecule on alcohol concentration, we also show data from the experiments of Ly et al. [28] in that figure. We obtain good agreement between all three data sets. Both simulation models as well as the experimental data exhibit a linear increase of the area per molecule with alcohol concentration. The agreement between the atomistic and the coarse-grained simulations is satisfactory. Only the coarse-grained simulations allow us to access to high alcohol concentrations due to the steep increase in equilibration times. The agreement between experiments and the coarse-grained model is reasonable considering the difference in systems. Re-optimization of the alcohol parameters both of the atomistic as well as the coarse-grained model will be made in order to reproduce experiments more exactly. The lipid parameters on the other hand are very appropriate for our studies. If we compare to experiments on pure DPPC in the bilayer state we are in very good agreement with the typical value of 63\AA^2 [49]. From our data we obtain an area expansion coefficient by linear regression of $\kappa = 14 \text{ nm}^2$ for the coarse-grained model in comparison to $\kappa = 8 \text{ nm}^2$ for the experiments. As we are only able to equilibrate low alcohol concentrations in the atomistic model we refrain from estimating this coefficient for the detailed model. This number measures the extrapolated difference between a bilayer in pure water against one in pure alcohol. This semiquantitative agreement between experiments and the coarse-grained model is in line with the recent conclusions that the same model can reproduce the phase coexistence in a mixed bilayer but the phase transition temperature is underestimated [41].

It is also of interest to determine where the butanol molecules are preferentially located within our system. This is deduced through density profiles which show a clear separation in a bilayer and a water phase. The headgroup area has the highest density and the center plane of the bilayer, which is its symmetry plane, is the plane of lowest density. This profile agrees very well with earlier atomistic and coarse-grained simulations [2, 40]. The butanol molecules are mainly located at the interface. This has previously been reported for ethanol and methanol [20, 22]. It is interesting to note that the butanol concentration in the bilayer interior is not zero. Atomistic detailed simulations of shorter

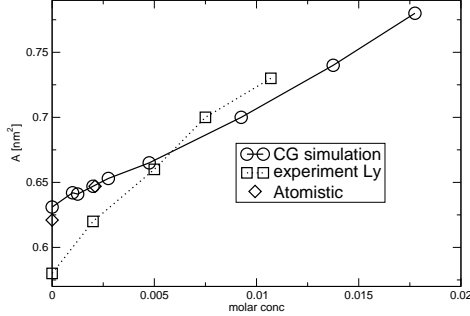


Figure 2: Area per molecule depending on butanol concentration comparing the atomistic and the coarse-grained model with experiments. Lines are meant as guide to the eye only. Note, that in the coarse grained simulations the concentrations are not the direct concentrations but renormalized according to the meaning of the water molecules (see text for details). The experimental data from ref. [28] are measured using another lipid (SOPC instead of DPPC). We estimate the errors in the atomistic simulations to be about 5% and in the coarse grained case to be about 2%.

alcohols have shown that methanol does not exist in the bilayer [22] and that ethanol was able to cross the bilayer but could not reside in it [22]. Generally, the probability of bilayer penetration increases with alcohol chain length due to the increasing hydrophobicity.

Comparing the coarse-grained with the atomistic model reveals some differences. First, it is clear that the atomistic density profile exhibits more details than can be represented in a coarse-grained model.

However, a more important difference between the models can be seen in the concentration of butanol in the water phase. The coarse-grained model overestimates the affinity of alcohols to the phase boundary. In contrast to the atomistic simulations the butanol concentration in the coarse-grained model vanishes almost in the water. Currently, the length of the atomistic simulation is too short to fully determine the extent of butanol penetration in the bilayer. In general, the coarse grained model can be used to make a basic sketch of the overall system features. However, future refinement is desirable. Figure 4 allows a more detailed investigation of the butanol position as we resolve the positions of the various sub-groups of the phospholipids along the bilayer normal. We see in both models that butanol stays in close contact to the lipid glycerol moiety. This is in agreement with earlier studies on shorter alcohols showing a strong hydrogen bonding of the alcohols to the oxygens in the glycerol [20, 22]. In the atomistic model we actually find the alcohol residing between the glycerol and the alkane tails whereas in our coarse-grained model the butanol and glycerol

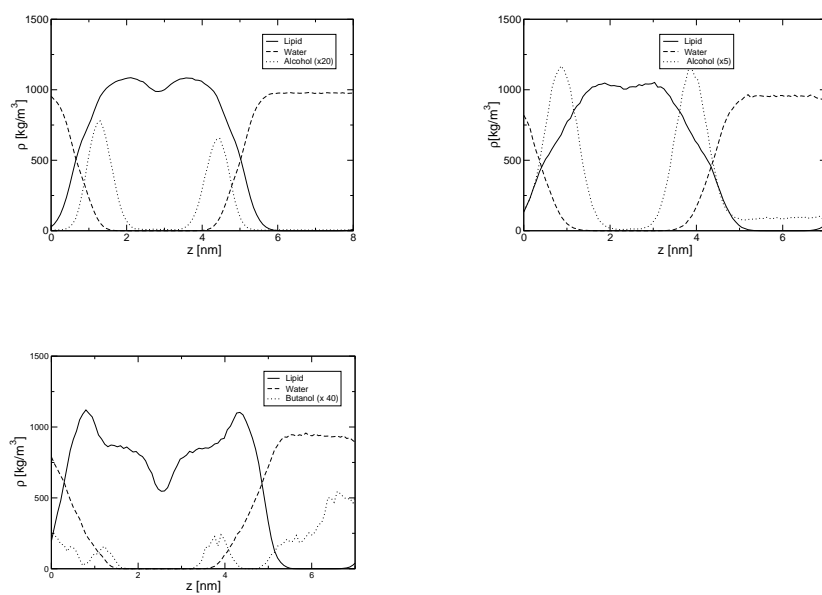


Figure 3: Density profile in coarse-grained and atomistic simulations. The upper panels represent coarse-grained simulations including 10 (left) or 100 (right) butanol molecules corresponding to molar concentrations of 0.0019 and 0.0189, respectively. The lower panel represents the atomistic data at a concentration of 0.0105. Note that for clarity the butanol concentration is multiplied by different factors as indicated in the figures.

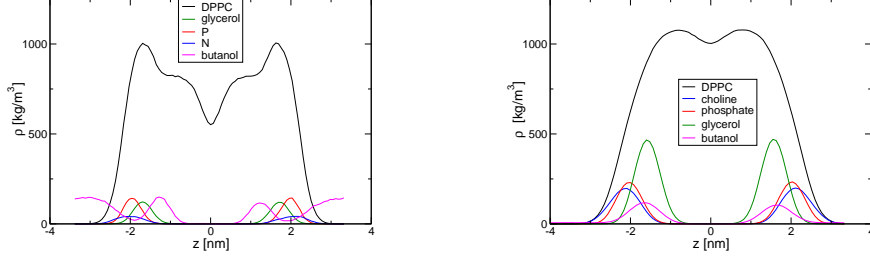


Figure 4: Density profiles of the bilayer, resolved according to the various groups in the lipids. Left: atomistic (concentration 0.0021), Right: coarse-grained (concentration 0.0019). Note that due to the equal weights of the coarse-grained groups the relative heights of the peaks cannot be directly compared.

layer coincide. Another important structural quantity where we obtain excellent agreement is the overall bilayer thickness. We use the distance between the phosphorus (or phosphate) planes as an indicator of thickness which leads to 3.96 nm in the atomistic case and 4.06 nm for the larger scale model. The latter number actually does not change at all if we use a butanol model where we exchange the water-like interaction of the OH group with an interaction site like the glycerols in the lipid.

If we compare the two concentrations of the coarse-grained model shown in Figure 3 we see that at the higher concentration the bilayer configuration becomes distorted at the interface. This occurs because the native interface cannot accommodate all alcohols. Additionally, the plane of lowest density is not as pronounced as it is with the lower concentration. This corresponds to experimental and simulational suggestions of increasing interdigitation between layers with alcohol concentration [39, 50, 51]. In order to quantify interdigitation we measured the density profiles of the alkane chains for the two leaflets separately. Figure 5 shows this data for three selected concentrations. At low concentrations there is no appreciable difference to the small interdigitation existing already in the pure bilayer. However, if we increase the concentration to about 2% mol of n-butanol we see clearly increased interdigitation. This indicates that that low butanol concentration has little impact on lipid structure. However, as the concentration increases the bilayer structure is massively changed but not abandoned.

The bilayer structure is often characterized using the deuterium order parameter which is defined as

$$-S_{CD} = \frac{2}{3}S_{xx} + \frac{1}{3}S_{yy}, \quad (1)$$

$$S_{\alpha\beta} = \langle 3 \cos \Theta_\alpha \cos \Theta_\beta - \delta_{\alpha\beta} \rangle, \quad \alpha, \beta = x, y, z \quad (2)$$

$$\cos \Theta_\alpha = \hat{e}_\alpha \hat{e}_z, \quad (3)$$

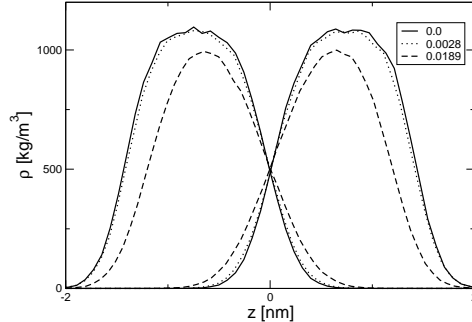


Figure 5: Density profiles for the alkane tails of the lipids from the coarse-grained simulations. The two leaflets are studied separately to examine the likelihood of interdigitation. All curves are shifted that the plane of equal density between the leaflets (symmetry plane of the bilayer) is at $z = 0$.

where \hat{e}_z is a unit vector in the laboratory z -direction and \hat{e}_α is a unit vector in the local coordinate system of the tails. The order parameter calculation is based on three connected carbons (or coarse-grained interaction sites) C_{i-1}, C_i , and C_{i+1} and $\vec{e} = \vec{r}_{i+1} - \vec{r}_{i-1}$. Figure 6 shows this order parameter. Since the coarse-grained chains are composed of four interaction centers, only two order parameters per chain can be defined. We see a slight difference in the order between the $sn - 1$ and $sn - 2$ chains where the $sn - 1$ chain is the alkane tail directly connected to the headgroup and $sn - 2$ is separated from the head group by the glycerol backbone.

With increasing concentration the order parameter decreases significantly at all positions along the chains. This is shown in the left-hand panel of Figure 6. The effect is independent of the distance from the headgroup and the identity of the chain ($sn - 1$ or $sn - 2$) as all the 4 curves in Figure 6 are parallel. This indicates that the alcohol not only influences the headgroup and its immediate vicinity but the whole layer. It is interesting to note that the coarse-grained model can distinguish between the two chains of the lipid, it actually overestimates the difference. The $sn - 1$ chain is more highly ordered in all cases. In order to directly compare the data between atomistic and coarse grained we assume that the four interaction sites in the lipid tails represent the four quarters of the DPPC tail not taking the glycerols into account. This means we take the middle atom of the second and third quarter of the atomistic tails (C_7 and C_{11}) to compare, these are shown as symbols in the left hand panel of figure 6. We see that for both atoms we get satisfactory agreement. Due to the intrinsic averaging of the coarse-grained model the difference between the models is about 10%. We could obtain better agreement if we used other atomistic carbons to

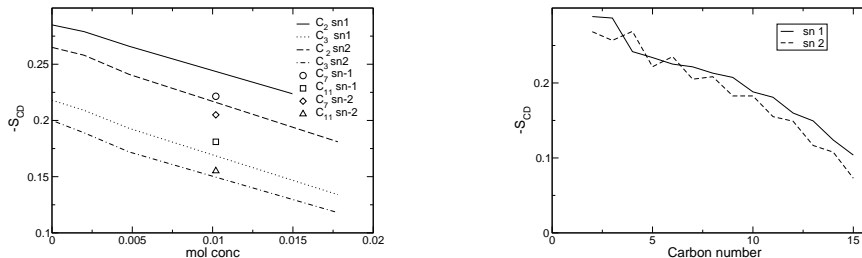


Figure 6: The left hand panel shows the dependence of the deuterium order parameter on alcohol concentration for coarse-grained and atomistic simulations. The atom numbers in the coarse-grained case represent the interaction sites with numbering starting at the head group. The right hand panel shows the deuterium order parameter for the individual lipid chains from the atomistic simulation at a molar n-butanol concentration of 0.0102.

directly compare. However, that would not be in the spirit of the used mapping. The right hand panel additionally shows the full atomistic order parameter for the case of the 0.0105 concentration (i.e. 39 alcohols).

4 Conclusion

In this study, we examined the effects of alcohol concentration on a lipid bilayer and showed that a coarse-grained model enables a wider range of parameters to be surveyed than is possible using only atomistic models. The accuracy of the coarse-grained model was examined by comparing experimentally important quantities with atomistic simulations and experimental data in a relatively short amount of computer time. This comparison indicated which coarse-grained parameters need to be refined.

The two models that we are comparing represent fundamentally the same system and the combination of the two can be used to investigate various bilayer properties. However, there are clear differences and a coarse-grained model should only be used with caution and in conjunction with an atomistic model as a basis. In this study we mainly see that the alcohol affinity to the actual interface is overestimated in the coarse-grained model. Nonetheless, most of the relevant properties are very well in agreement between the two models. We will continue evaluating bilayer properties for both models. From these studies, we will be able to identify important parameters that should be incorporated into future coarse-grained models. For the results here the exact coarse grained interactions were not very important as we performed additional simulations with slightly changed parameters and obtained the same conclusions.

We showed that increasing alcohol concentration leads to a linear increase

of the area per molecule and to a linear decrease in the chain order parameter. The alcohols are modeled as amphiphilic molecules and tend to reside at the interface, i.e. between the headgroup and the tails. Butanols are more likely to enter the tail region shorter alcohols. At high butanol concentrations, the interface can become saturated and cause butanol molecules to return to the water phase. Lipid conformational changes increase with alcohol concentration and this corresponds to an increase in leaflet interdigitation.

References

- [1] Feller, S. E.; Zhang, Y. H.; Pastor, R. W.; J Chem Phys 1995; 103, 10267–10276.
- [2] Tieleman, D. P.; Marrink, S. J.; Berendsen, H. J. C.; Biochim Biophys Acta Rev on Biomem 1997; 1331, 235–270.
- [3] Tobias, D. J.; Tu, K.; Klein, M. L.; Curr Opin in Coll Int Sc 1997; 2, 15–27.
- [4] Bandyopadhyay, S.; Tarek, M.; Klein, M. L.; Curr Opin in Coll Int Sc 1998; 3, 242–246.
- [5] Husslein, T.; Newns, D. M.; Pattnaik, P. C.; Zhong, Q.; Moore, P. B.; Klein, M. L.; J Chem Phys 1998; 109, 2826–2832.
- [6] Rog, T.; Pasenkiewicz-Gierula, M.; Biophys J 2001; 81, 2190–2202.
- [7] Saiz, L.; Klein, M. L.; J Chem Phys 2002; 116, 3052–3057.
- [8] Patra, M.; Karttunen, M.; Hyvönen, M.; Falck, E.; Lindqvist, P.; Vattulainen, I.; Biophys J 2003; 84, 3636–3645.
- [9] Patra, M.; Karttunen, M.; Hyvönen, M. T.; Falck, E.; Vattulainen, I.; J Phys Chem B 2004; 108, 4485–4494.
- [10] Leontiadou, H.; Mark, A. E.; Marrink, S. J.; Biophys J 2004; 86, 2156–2164.
- [11] Mashl, R. J.; Scott, H. L.; Subramaniam, S.; Jakobsson, E.; Biophys J 2001; 81, 3005–3015.
- [12] Gurtovenko, A.; Patra, M.; Karttunen, M.; Vattulainen, I.; Biophys J 2004; 86, 3461–3472.
- [13] Pandit, S. A.; Bostick, D.; Berkowitz, M. L.; Biophys J 2003; 85, 3120–3131.
- [14] Balali-Mood, K.; Harroun, T. A.; Bradshaw, J. P.; Eur Phys J E 2003; 12, S135–S140.
- [15] de Vries, A. H.; Mark, A. E.; Marrink, S. J.; J Phys Chem B 2004; 108, 2454–2463.

- [16] Tu, K.; Klein, M. L.; Tobias, D. J.; *Biophys J* 1998; 75, 2147–2156.
- [17] Smondryev, A. M.; Berkowitz, M. L.; *Biophys J* 2000; 78, 1672–1680.
- [18] Pandit, S. A.; Bostick, D.; Berkowitz, M. L.; *Biophys J* 2004; 86, 1345–1356.
- [19] Falck, E.; Patra, M.; Karttunen, M.; Hyvonen, M. T.; Vattulainen, I.; *Biophys J* 2004; 87, 1076–1091.
- [20] Feller, S. E.; Brown, C. A.; Nizza, D. T.; Gawrisch, K.; *Biophys J* 2002; 82, 1396–1404.
- [21] Bemporad, D.; Essex, J. W.; Luttmann, C.; *J Phys Chem B* 2004; 108, 4875–4884.
- [22] Patra, M.; Vattulainen, I.; Salonen, E.; Terama, E.; Faller, R.; Lee, B. W.; Holopainen, J.; Karttunen, M.; Under the influence of alcohol: The effect of ethanol and methanol on lipid bilayers; 2004; submitted
- [23] Sum, A. K.; Faller, R.; de Pablo, J. J.; *Biophys J* 2003; 85, 2830–2844.
- [24] Pereira, C. S.; Lins, R. D.; Chandrasekhar, I.; Carlos, L.; Freitas, G.; Hünenberger, P. H.; *Biophys J* 2004; 86, 2273–2285.
- [25] Smondryev, A. M.; Berkowitz, M. L.; *Biophys J* 1999; 76, 2472–2478.
- [26] Sum, A. K.; de Pablo, J. J.; *Biophys J* 2003; 85, 3636–3645.
- [27] Ly, H. V.; Block, D. E.; Longo, M. L.; *Langmuir* 2002; 18, 8988–8995.
- [28] Ly, H. V.; Longo, M. L.; *Biophys J* 2004; 87, 1013–1033.
- [29] Bisson, L. F.; Block, D. E.; in Ciani, M., ed., *Biodiversity and Biotechnology of Wine Yeasts*; Kerala: Research Signpost; 2002; pp. 85–98.
- [30] Cramer, A. C.; Vlassides, S.; Block, D. E.; *Biotechnol Bioeng* 2002; 77, 49–60.
- [31] Smit, B.; Hilbers, P. A. J.; Esselink, K.; Rupert, L. A. M.; van Os, N. M.; Schlijper, A. G.; *Nature* 1990; 348, 624–625.
- [32] Goetz, R.; Gompper, G.; Lipowsky, R.; *Phys Rev Lett* 1999; 81, 221–224.
- [33] Mouritsen, O. G.; in Pasini, P.; Zannoni, C., eds., *Advances in the Computer Simulation of Liquid Crystals*; NATO; Dordrecht: Kluwer; vol. C 545 of *NATO ASI*; 2000; pp. 139–188.
- [34] Soddemann, T.; Dünweg, B.; Kremer, K.; *Eur Phys J E* 2001; 6, 409–419.
- [35] Shelley, J. C.; Shelley, M. Y.; Reeder, R. C.; Bandyopadhyay, S.; Klein, M. L.; *J Phys Chem B* 2001; 105, 4464–4470.

- [36] Ayton, G.; Voth, G. A.; *Biophys J* 2002; 83, 3357–3370.
- [37] Guo, H.; Kremer, K.; *J Chem Phys* 2003; 118, 7714–7723.
- [38] Müller, M.; Katsov, K.; Schick, M.; *J Polym Sci Part B Polym Phys* 2003; 41, 1441–1451.
- [39] Kranenburg, M.; Venturoli, M.; Smit, B.; *J Phys Chem B* 2003; 107, 11491–11501.
- [40] Marrink, S. J.; de Vries, A. H.; Mark, A.; *J Phys Chem B* 2004; 108, 750–760.
- [41] Faller, R.; Marrink, S.-J.; *Langmuir* 2004; 20, 7686–7693.
- [42] Lindahl, E.; Hess, B.; van der Spoel, D.; *J Mol Model* 2001; 7, 306–317.
- [43] Berendsen, H. J. C.; Postma, J. P. M.; van Gunsteren, W. F.; DiNola, A.; Haak, J. R.; *J Chem Phys* 1984; 81, 3684–3690.
- [44] Berger, O.; Edholm, O.; Jahnig, F.; *Biophys J* 1997; 72, 2002–2013.
- [45] Berendsen, H. J. C.; Grigera, J. R.; Straatsma, T. P.; *J Phys Chem* 1987; 91, 6269–6271.
- [46] Essmann, U.; Berkowitz, M. L.; *Biophys J* 1999; 76, 2081–2089.
- [47] Lee, B. W.; Faller, R.; Sum, A. K.; Vattulainen, I.; Patra, M.; Karttunen, M.; *Fluid Phase Equilibria* 2004; 225, 63–68.
- [48] Marrink, S.-J.; MANUAL: Coarse Grained Model for Semi-Quantitative Lipid Simulations; Version 1.4; available at <http://md.chem.rug.nl/marrink/coarsegrain.html>.
- [49] Nagle, J. F.; Tristram-Nagle, S.; *Curr Opin Struct Biol* 2002; 10, 474–480.
- [50] Mou, J. X.; Yang, J.; Huang, C.; Shao, Z. F.; *Biochemistry* 1994; 33, 9981–9985.
- [51] Adachi, T.; Takahashi, H.; Ohki, K.; Hatta, I.; *Biophys J* 1995; 68, 1850–1855.